Macedonian Journal of Chemistry and Chemical Engineering, Vol. **32**, No. 2, pp. 239–250 (2013)
ISSN 1857-5552
UDC: 547.587.51

MJCCA9 – 623
Received: December 18, 2012
Accepted: April 10, 2013

Original scientific paper

SYNTHESIS AND STRUCTURE OF *(R,S)*-2-METHYL-4-(4-NITROPHENYL)-PYRANO[3,2-*c*] CHROMEN-5(4*H*)-ONE

Rosica P. Nikolova[1], Boris Shivachev[1], Bozhana Mikhova[2], Bistra Stamboliyska[2], Kristina Mladenovska[3], Ana P. Panovska[3], Emil Popovski[4]*

[1]*Institute of Mineralogy and Crystallography, Bulgarian Academy of Sciences, Acad. G. Bonchev Str., Build. 107, 1113 Sofia, Bulgaria*
[2]*Institute of Organic Chemistry with Centre of Phytochemistry, Bulgarian Academy of Sciences, Acad. G. Bonchev Str., Build. 9, 1113 Sofia, Bulgaria*
[3]*Department of Drug Design and Metabolism, Faculty of Pharmacy, Ss. Cyril and Methodius University, Vodnjanska 17, 1000 Skopje, R. Macedonia*
[4]*Institute of Chemistry, Faculty of Natural Sciences and Mathematics, Ss. Cyril and Methodius University, Arhimedova 5, 1000 Skopje, PO Box 162, R. Macedonia*
popovski.emil@gmail.com

In this paper, the synthesis and structure of a novel pyrano[3,2-c]coumarin, which was obtained unexpectedly in a reaction of phosphoryl chloride and acenocoumarol, are presented. The chemical structure of the novel compound was elucidated by a detailed spectroscopic analysis based mainly on 1D and 2D NMR techniques. The structure was finally confirmed with a single-crystal X-ray analysis. The B3LYP/6-311+G** method correctly reproduces the bond lengths, bond angles, torsion angles, and other experimental spectroscopic data, which can be useful for investigating the characteristics of some structurally related molecules. Additionally, the title compound was obtained in high yields by performing a dehydratation reaction of acenocuomarol with acetic anhydride.

Keywords: acenocoumarol; pyrano[3,2-c]coumarin; crystal structure; DFT calcualations

СИНТЕЗА И СТРУКТУРА НА (*R,S*)-2-МЕТИЛ-4-(4-НИТРОФЕНИЛ)-ПИРАНО[3,2-*c*]ХРОМЕН-5(4*H*)-ОН

Во овој труд се опишани синтезата и структурата на еден нов пирано[3,2-c]кумарин кој беше добиен неочекувано во реакција на фосфорилхлорид и аценокумарол. Хемиската структура на новото соединение беше определена со детална спектроскопска анализа базирана главно на 1D и 2D NMR техниките. Структурата конечно беше потврдена и со рендгенска анализа на монокристалот на добиеното соединение. Методата B3LYP/6-311+G** коректно ги репродуцира должините на врските, аглите на врските и торзионите агли, како и другите експериментални спектроскопски податоци и може да биде корисна при истражувањата на карактеристиките на соединенија со слична структура. Дополнително, новото соединение беше добиено со висок принос со примена на реакција на дехидратација на аценокумарол со анхидрид на оцетна киселина.

Клучни зборови: аценокумарол; пирано[3,2-c]кумарин; кристална структура; DFT пресметки

1. INTRODUCTION

Coumarins and their derivatives are an important class of compounds in medicinal chemistry, with expansive spectra of biological activity. An enormous number of articles reports on diverse synthetic or natural substances with coumarine scaffold that exhibit anticoagulant, anti-HIV, and anticancer properties and capability for many other biological activities. On the other hand, derivatives of pyran have also gathered significant attention of organic and medicinal chemists for many years due to their biological and pharmaceutical properties. These two moieties (coumarin and pyran) being in the same molecule is characteristic of pyranocoumarins, an important class of compounds that are currently in the scientific focus of many research groups. Pyranocoumarins, either from natural, semisynthetic, or synthetic origin, possess antibacterial [1–3], antifungal [4–5], anticoagulant [6–7], anti-HIV [8], antiproliferative [9–10], and anticancer [11] properties and can perform other activities [12–15]. For these reasons, organic chemists have strived to find more efficient synthetic routes to known or novel pyranocoumarins [16–21].

In this paper we present the synthesis and structure of a novel pyrano[3,2-c]coumarin, which was obtained unexpectedly in a reaction of phosphoryl chloride and acenocoumarol (**3**), one of the most widely used oral anticoagulant in the last two decades.

2. EXPERIMENTAL

(*R,S*)-acenocoumarol and other chemicals were purchased commercially and used without further purification.

The melting point was determined on a Reichert hot-stage apparatus and was uncorrected.

The 1D and 2D (COSY, HMQC, and HMBC) NMR spectra were run on a Bruker DRX-250 spectrometer in DMSO-d_6 solvent using a standard Bruker software. The residual solvent signal was used as an internal standard for the ^{1}H (δ = 2.5 ppm) and ^{13}C (δ = 39.5 ppm) NMR spectra.

The FTIR spectra (4000–400 cm^{-1}) were recorded on Perkin-Elmer System 2000 at ambient temperature using KBr pellets.

Diffraction data were collected at room temperature by the ω-scan technique, on an Agilent Diffraction SuperNova Dual four-circle diffractometer equipped with an Atlas CCD detector using mirror-monochromatized MoKα radiation from a microfocus source (λ = 0.7107 Å). The determination of cell parameters, data integration, scaling, and absorption correction were carried out using the CrysAlisPro program package [22]. The structures were solved by direct methods (SHELXS-97) and refined by full-matrix least-square procedures on F^2 (SHELXL-97) [23]. The non-hydrogen atoms were refined anisotropically, and hydrogen atoms were placed at idealized positions and refined using the riding model. A summary of the fundamental crystal and refinement data is provided in Table 1.

The quantum chemical calculations were performed using the Gaussian 09 package [24] on a MADARA grid. The geometry optimizations of the structures investigated were done without symmetry restrictions, using density functional theory (DFT). We employed the B3LYP hybrid functional, which combines Becke's three-parameter nonlocal exchange with the correlation functional of Lee et al. [25, 26], adopting 6-311+G(d,p). The stationary points found on the molecular potential energy hypersurfaces were characterized using standard harmonic vibrational analysis. The absence of imaginary frequencies confirmed that the stationary points corresponded to minima on the potential energy hypersurfaces. For a better correspondence between the experimental and calculated values, we modified the results using empirical scaling factors [27]. ^{1}H and ^{13}C-NMR chemical shifts of 6 and of the solvent DMSO-d6 were calculated by using the GIAO method [28] at the same level of theory (reference compound TMS was calculated at the same level).

T a b l e 1

Important crystallographic and refinement details for compound 6

$C_{19}H_{13}NO_5$	$\theta_{max} = 29.0°$, $\theta_{min} = 3.0°$
Mw = 335.30	*h* = −18 17
Orthorhombic, *Pbcn*	*k* = −9 9
a = 13.7944 (4) Å	*l* = −41 38
b = 7.4249 (3) Å	*R*int = 0.035
c = 30.4072 (12) Å	Refinement on *F*2
V = 3114.4 (2) Å3	Least-squares matrix: full
Z = 8	$R[F2 > 2\sigma(F2)] = 0.063$
*D*x = 1.430 Mg m−3	*wR*(*F*2) = 0.184
Mo*K*α radiation, λ = 0.7107 Å	*S* = 1.05
μ = 0.11 mm^{-1}	3795 reflections
T = 290 K	227 parameters
Prism, colorless, 0.26 × 0.21 × 0.20 mm	0 restraints
SuperNova, Dual, Cu at zero, Atlas diffractometer	Secondary atom site location: difference Fourier map
Radiation source: SuperNova (Mo) X-ray Source	Hydrogen site location: inferred from neighboring sites
Monochromator: mirror	H-atom parameters constrained
Detector resolution: 10.3974 pixels mm^{-1}	$w = 1/[\sigma^2(F_o^2) + (0.0645P)^2 + 2.0276P]$ where $P = (F_o^2 + 2F_c^2)/3$
ω scans	$(\Delta/\sigma)_{max} < 0.001$
Absorption correction: multiscan *CrysAlisPro*, Agilent Technologies	$\Delta\rho_{max} = 0.25$ e $Å^{-3}$
$T_{min} = 0.832$, $T_{max} = 1.000$	$\Delta\rho_{min} = -0.21$ e $Å^{-3}$
3795 independent reflections	Extinction correction: none
2336 reflections with $I > 2\sigma(I)$	

2.1. *Synthesis of* (*R,S*)*-2-methyl-4-*(*4-nitrophenyl*)*pyrano*[*3,2-c*]*chromen-5-one* (***6***)

Method A. The mixture of 2 g (*R,S*)-acenocoumarol (**3**) and 20 ml phosphoryl chloride was heated at 70 °C for 4 h. Afterward, the reaction mixture was cooled to room temperature, then slowly poured onto crushed ice and stirred for 45 min. Crystals of **6** were formed, separated by filtration, and washed with cold water.

Method B. In 40 ml of acetic anhydride, 2 g of **3** was dissolved. To the solution, 2–3 drops of concentrated sulfuric acid were added and stirred for 1 h. The colorless crystals were collected by simple vacuum filtration and washed with a large quantity of water. The typical yield of the crude product was about 85%. The purification was performed by recrystallization, first with dioxane and afterward with ethanol. The melting point of pure crystals was 208 °C.

^{1}H-NMR (250 MHz, DMSO-*d*6) *δ*/ppm: 8.16 (2H, d, *J* = 8.0 Hz, H-23 and H-25), 7.90 (1H, dd, *J* = 8.0, 1.5 Hz, H-6), 7.70 (1H, ddd, *J* = 8.0, 8.0, 1.5 Hz, H-8), 7.57 (2H, d, *J* = 8.0 Hz, H-22 and H-26), 7.5–7.4 (2H, overlapped, H-7 and H-9), 5.20 (1H, dq, *J* = 4.3, 1.0 Hz, H-2), 4.63 (1H, dq, *J* = 4.3, 1.0 Hz, H-1), 2.05 (3H, br s, CH_3-31).

3. RESULTS AND DISCUSSION

In our previous work, it has been shown that 4-hydroxycoumarin (**1**) can be simply transformed into 4-aminocoumarin (2) *via* solvent free reaction (Figure 1) [29].

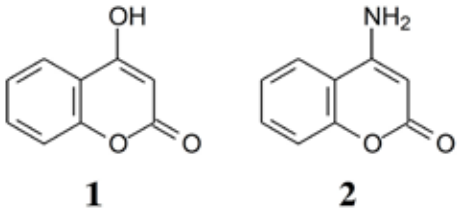

Fig. 1. Structure of 4-hydroxycoumarin (**1**) and 4-aminocoumarin (**2**)

Motivated by this finding, the primary target of this work was to replace the hydroxyl group in **3** with an amino group to obtain (*R,S*)-4-amino-3-[1-(4-nitrophenyl)-3-oxobutyl]-2H-chromen-2-one (**5**). Due to the electronic similarity of oxygen (hydroxyl group) and nitrogen (amino group), we supposed that **5** could be a potential bioisostere of the well-known anticoagulant. However, this reaction failed in the case of **3** (Scheme 1). As a second choice, the reaction of **3** with phosphoryl chloride was performed to obtain (*R,S*)-4-chloro-3-[1-(4-nitrophenyl)-3-oxobutyl]-2H-chromen-2-one (**4**). Subsequently, the targeted compound **5** was expected to be obtained in a nucleophilic reaction of ammonia with intermediate **4** (Scheme 1). However, an unplanned cyclization occurred, resulting in the formation of (*R,S*)-2-methyl-4-(4-nitrophenyl)pyrano[3,2-c]chromen-5-one (**6**). The reaction was performed at three different temperatures (70 ºC, 90 ºC, and boiling temperature of phosphoryl chloride) in order to obtain and isolated **4**. However, in all the reaction conditions, the compound **6** was obtained as a product. The yield of the crude product was ~60%, and the impurity of the crystals was significant. Because no literature data was found for this compound, an attempt for an efficient synthesis of **6** was made. Since the unexpected cyclization of **3** was some kind of a dehydration reaction, product **6** was obtained with a high yield in the reaction of **3** with acetic anhydride (Scheme 1).

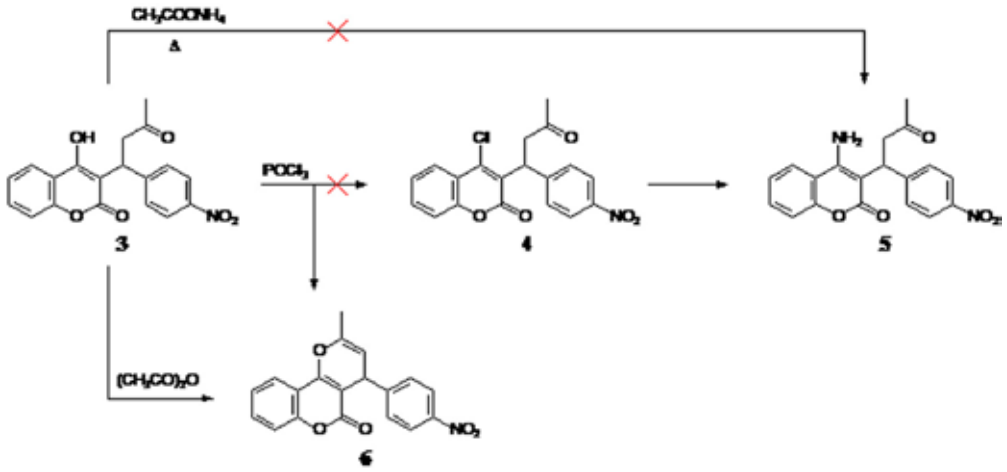

Scheme 1. Planned but unsuccessful reactions and unexpected product

In the NMR spectra, characteristic signals for a coumarin moiety and a *p*-nitrophenyl group were visible. However, the expected signal for a CH_2 group for compound 5 was lacking. An oxygenated carbon (C4 according to Figure 2) at the coumarin with signal at δ 156.1 and a –MeC=CH– fragment could be confirmed by the positions of the signals at δ 18.0; 2.05 (=CCH_3), 146.0 (C=), and 102.7; 5.20 (CH=) in the ^{13}C and ^{1}H spectra, respectively. The correlations between the signal at 5.20 with the signals of CH_3, C3, and C2, as well as between the signal

at 4.63 with the signal of C4 in the HMBC spectra, confirmed the suggested structure as **6**.

Crystals of **6** suitable for the single-crystal X-ray analysis were grown by slow evaporation from ethanol. Compound 6, $C_{19}H_{13}NO_5$, crystallizes in the centrosymmetric *Pbcn* space group with one molecule per asymmetric unit (Figure 2). The structural features (bond distances and angles) of the molecule present in the ASU are comparable to those of similar compounds [30–32] (Table 2 and Table 3). The phenyl moiety is nearly planar (rms of 0.011(4) Å). The NO_2 group also lies in a plane of the phenyl ring's mean planes (torsion angles of O11-N11-C24-C23 and O12-N11-C24-C23 are –0.24º and –178.14º, respectively).

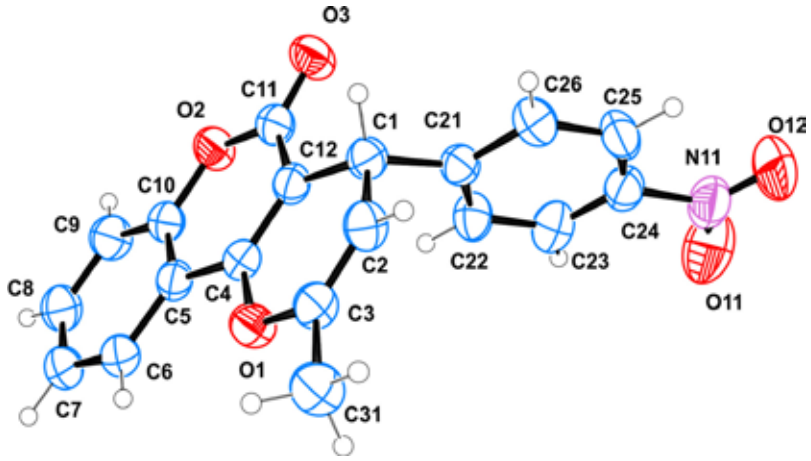

Fig. 2. Single-crystal X-ray structure of **6**. Displacement ellipsoids are drawn at the 50 % probability level (the hydrogen atoms are represented by circles of arbitrary radii)

T a b l e 2

Bond lengths (Å) for 6 determined by X-ray diffraction and DFT calculations[a]

Parameter	X-ray	B3LYP	Parameter	X-ray	B3LYP
O_1—C_4	1.358 (3)	1.356	C_{21}—C_{26}	1.391 (3)	1.399
O_1—C_3	1.402 (3)	1.396	C_{21}—C_1	1.529 (3)	1.534
O_2—C_{10}	1.379 (3)	1.363	C_1—C_2	1.512 (3)	1.510
O_2—C_{11}	1.382 (3)	1.391	C_6—C_7	1.374 (4)	1.380
C_{12}—C_1	1.508 (3)	1.516	C_9—C_8	1.377 (4)	1.394
C_{12}—C_4	1.354 (3)	1.359	C_9—C_{10}	1.386 (4)	1.399
C_{12}—C_{11}	1.442 (3)	1.455	C_7—C_8	1.382 (4)	1.388
O_3—C_{11}	1.205 (3)	1.206	C_{24}—C_{23}	1.364 (4)	1.400
C_5—C_4	1.445 (3)	1.445	C_{24}—C_{25}	1.371 (5)	1.459
C_5—C_6	1.402 (3)	1.405	C_{24}—N_{11}	1.483 (4)	1.392
C_5—C_{10}	1.396 (3)	1.402	C_{26}—C_{25}	1.381 (4)	1.389
C_2—C_3	1.310 (3)	1.321	C_{26}—C_{25}	1.395 (4)	1.390
C_3—C_{31}	1.483 (4)	1.492	N_{11}—O_{12}	1.218 (4)	1.225
C_{21}—C_{22}	1.383 (4)	1.396	N_{11}—O_{12}	1.224 (4)	1.226

[a]For atom numbering, see Figure 2.

Table 3

Selected bond angles (°) for 6 determined by X-ray diffraction and DFT calculations

Parameter	X-ray	B3LYP	Parameter	X-ray	B3LYP
C_4—O_1—C_3	117.5 (18)	118.4	C_2—C_1—C_{21}	107.5 (19)	111.7
C_{10}—O_2—C_{11}	121.4 (19)	122.5	C_3—C_2—C_1	124.2 (2)	123.8
C_4—C_{12}—C_{11}	119.7 (2)	119.9	C_7—C_6—C_5	120.2 (3)	120.2
C_4—C_{12}—C_1	122.6 (2)	122.1	C_8—C_9—C_{10}	119.0 (3)	119.1
C_{11}—C_{12}—C_1	117.7 (2)	117.9	C_6—C_7—C_8	120.0 (3)	120.0
C_6—C_5—C_4	124.6 (2)	124.2	C_{23}—C_{24}—C_{25}	122.1 (3)	121.8
C_6—C_5—C_{10}	118.7 (2)	118.9	C_{23}—C_{24}—N_{11}	119.1 (3)	119.0
C_{10}—C_5—C_4	116.7 (2)	118.9	C_{25}—C_{24}—N_{11}	118.7 (3)	119.1
C_{12}—C_4—O_1	123.7 (2)	123.1	O_2—C_{10}—C_9	116.9 (2)	117.3
C_{12}—C_4—C_5	122.0 (2)	121.7	O_2—C_{10}—C_5	121.9 (2)	121.6
O_1—C_4—C_5	114.3 (2)	115.1	C_9—C_{10}—C_5	121.1 (2)	121.0
C_2—C_3—C_{31}	127.4 (2)	127.5	C_{23}—C_{22}—C_{21}	121.2 (3)	121.0
O_1—C_3—C_{31}	110.0 (2)	110.4	C_{21}—C_{26}—C_{25}	120.3 (3)	120.9
C_{22}—C_{21}—C_1	122.0 (2)	120.6	C_9—C_8—C_7	120.9 (3)	120.7
C_{26}—C_{21}—C_1	119.0 (2)	120.3	O_{12}—N_{11}—O_{11}	125.6 (3)	124.5
O_3—C_{11}—O_2	116.3 (2)	117.6	O_{12}—N_{11}—C_{24}	117.2 (4)	117.7
O_3—C_{11}—C_{12}	125.4 (2)	125.1	O_{11}—N_{11}—C_{24}	117.1 (3)	117.7
O_2—C_{11}—C_{12}	118.3 (2)	117.1	C_{24}—C_{23}—C_{22}	118.9 (3)	118.6
C_{12}—C_1—C_2	108.2 (2)	108.8	C_{24}—C_{25}—C_{26}	118.7 (3)	118.7
C_{12}—C_1—C_{21}	114.9 (2)	112.9			

Table 4

Selected torsion angles (°) for 6 determined by X-ray diffraction and DFT calculations

Parameter	X-ray	B3LYP	Parameter	X-ray	B3LYP
C_{11}—C_{12}—C_4—O_1	179.4(2)	175.1	C_{21}—C_1—C_2—C_3	–111.3(3)	–112.6
C_1—C_{12}—C_4—O_1	–0.6(4)	–3.1	C_{10}—C_5—C_6—C_7	1.2(4)	0.3
C_{11}—C_{12}—C_4—C_5	0.1(4)	4.3	C_4—C_5—C_6—C_7	–178.1(2)	–179.2
C_1—C_{12}—C_4—C_5	–179.9(2)	–177.3	C_5—C_6—C_7—C_8	0.4(4)	–0.1
C_3—O_1—C_4—C_{12}	7.5(3)	7.8	C_{11}—O_2—C_{10}—C_9	–179.5(2)	–179.9
C_3—O_1—C_4—C_5	–173.1(2)	–171.6	C_{11}—O_2—C_{10}—C_5	–0.3(4)	–0.5
C_{10}—C_5—C_4—C_{12}	2.2(4)	1.1	C_0—C_9—C_{10}—O_2	–179.1(3)	–179.3
C_6—C_5—C_4—C_{12}	–178.5(2)	–178.3	C_8—C_9—C_{10}—C_5	1.7(4)	0.1
C_{10}—C_5—C_4—O_1	–177.2(2)	–178.3	C_6—C_5—C_{10}—O_2	178.6(2)	179.1
C_6—C_5—C_4—O_1	2.1(3)	2.1	C_4—C_5—C_{10}—O_2	–2.0(4)	–1.3
C_4—O_1—C_3—C_2	–3.2(4)	–8.4	C_6—C_5—C_{10}—C_9	–2.3(4)	–0.3
C_4—O_1—C_3—C_{31}	176.7(2)	171.2	C_4—C_5—C_{10}—C_9	177.1(2)	179.2
C_{10}—O_2—C_{11}—O_3	–178.0(2)	–177.0	C_{26}—C_{21}—C_{22}—C_{23}	0.4(4)	0.1

Typical hydrogen bonding interactions could not be located in the structure of **6**. However, a fused ring system (pyrano[3,2-c] chromen-5(4H)-one) and a nitrobenzene moiety are in the base of the observed C–H···π and C–H···O interactions (Figure 3). In order to maximize the 3D stabilization, the $N^+O_2^-$ group is surrounded by CH_3 and a phenyl ring, allowing the formation of CH_3···O and $C–H_{aromatic}$···O interactions (Figure 4). Thus, the resulting network of weak interactions is three-dimensional, producing undulating layers along *b,* while pore channels (d = 2.24 Å) can be observed along *c* (Figure 5).

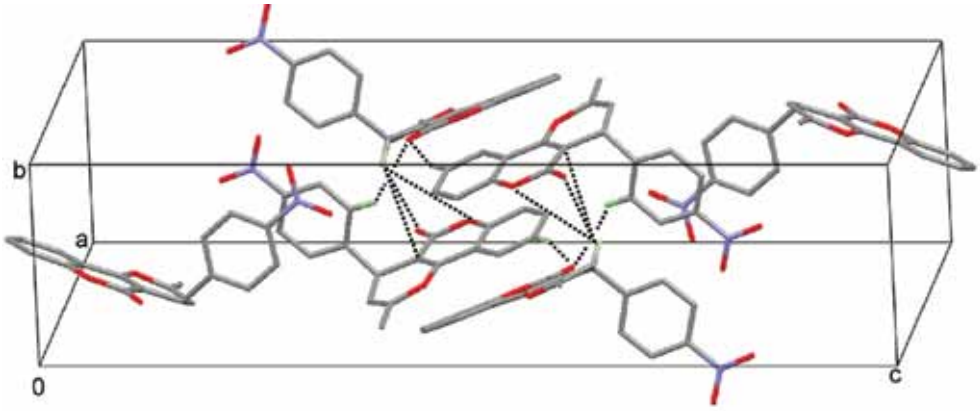

Fig. 3. Crystal-packing diagram of **6**, showing the weak π interactions involving the fused ring system (the interactions are indicated by dashed lines)

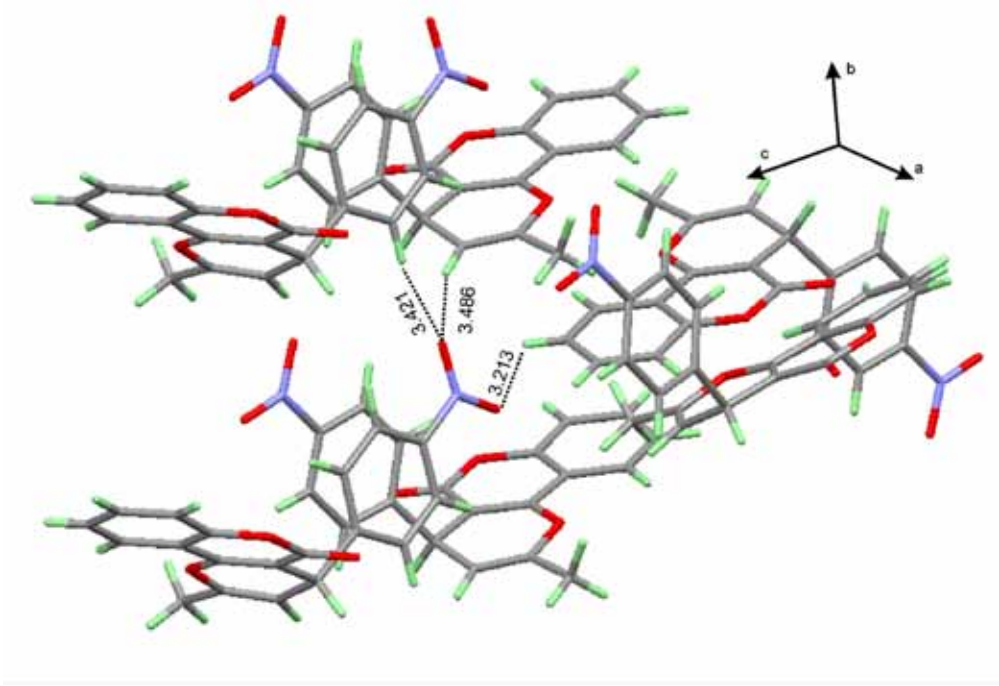

Fig. 4. Part of the crystal structure of **6**, showing NO_2 surrounding and C–H···O interactions (indicated by dashed lines)

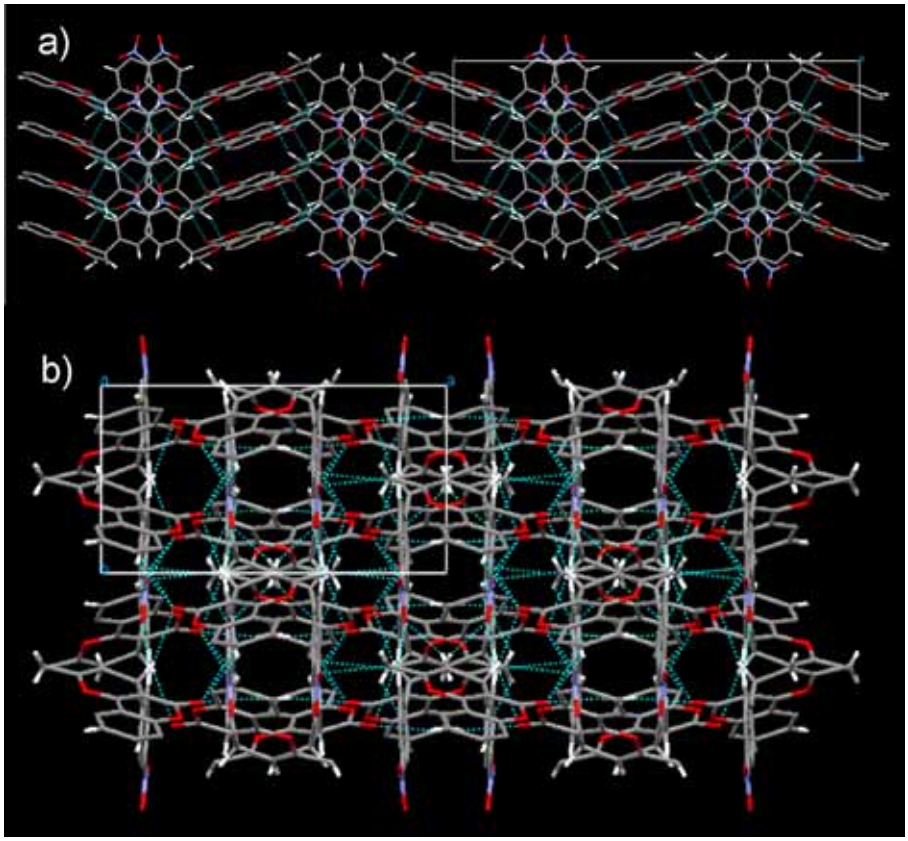

Fig. 5. The three-dimensional arrangement of the molecules in the crystal, (a) producing undulating layers along *b* and (b) pore channels (with diameter of 2.24 Å) d along *c*

3.1. *Optimized structures*

The molecular structure of compound **6** in the ground state (in vacuo) was optimized using DFT. In accordance with the X-ray diffraction, the theory used predicts that the studied molecule is composed of atoms lying approximately in two planes: one of the phenyl rings with an NO_2 group as a substituent and the other of coumarine containing moiety. The optimized parameters (bond lengths, bond angles, torsion angles) were compared with the experimental data for the title compound in Table 2, Table 3, and Table 4. As one can see, there is a quite satisfactory agreement between the calculated structures and the experimentally determined X-ray crystal structure. On the other hand, no one could expect a full coincidence between the experimental data for the crystal state and theoretical values, computed for an isolated molecule. The biggest difference between the experimental and calculated bond lengths was about 0.028 Å. The mean absolute deviation (MAD) was found to be 0.009 Å, indicating that the bond lengths obtained by the B3LYP method show a strong correlation with experimental values. For bond angles, the biggest difference and the MAD were about 1.9 and 0.5, respectively.

IR spectrum calculations were performed to determine the types of molecular motions associated with each of the observed experimental bands. The agreement between the calculated frequencies and the experimental data was very good. The mean absolute deviation between experimental ($\nu_{exp.}$) and theoretical ($\nu_{theor.}$) values was 6.6 cm^{-1}. Selected numeric values of measured frequencies together with calculated frequencies, intensities, and assignments are presented in Table 5.

Table 5

The selected measured infrared band positions (cm^{-1}), vibrational wave numbers (cm^{-1}), infrared intensities ($km \cdot mol^{-1}$), and their tentative assignments

ν_{calc} [a]	$A_{calc.}$	$\nu_{exp.}$		Assignment[b]	ν_{calc} [a]	$A_{calc.}$	$\nu_{exp.}$		Assignment[b]
1726	577.1	1716	*vs*	$\nu_{C=O}$	1152	78.2	1155	*m*	ν_{C-Ph}
1697	33.1			$\nu_{C_2=C_3}$	1127	56.5	1105	*m*	ν_{C-CH_3}
1607	167.2	1627	*s*	$\nu_{C_4=C_{12}}$	1084	63.8	1083	*x*	ν_{CN}
1594	40.8	1607	*m*	ν_{CC}^{Coum}	1036	1.2	1030	*m*	δ_{CH_3}
1593	47.6	1595	*m*	ν_{CC}^{Ph}	1003	94.7	1013	*x*	$\nu_{O_1C_9}$
1584	31.3	1577	*x*	ν_{CC}^{Ph}	1000	7.8	991	*x*	δ_{HCC}^{Ph}
1554	38.4			ν_{CC}^{Coum}	970	0.0	972	*x*	δ_{COO_1}
1526	229.0	1513	*s*	$\nu_{NO_2}^{as}$	883	24.0	899	*m*	$\delta_{O-C=O}$
1479	11.3	1493	*m*	δ_{HCC}^{Ph}	853	4.7	872	*x*	γ_{CCH}^{Coum}
1471	28.3	1458	*m*	δ_{HCC}^{Coum}	852	0.5	852	*x*	δ_{CCC}^{Ph}
1442	6.9			δ_{CH_3}	845	41.7	837	*m*	γ_{CCH}^{Ph}
1436	19.6	1434	*x*	δ_{HCC}^{Coum}	842	9.0			γ_{CCH}^{Ph}
1426	5.3	1419	*x*	δ_{CH_3}	832	83.1	833	*m*	δ_{ONO}
1404	19.2	1392	*s*	ν_{CH}^{Ph}	821	1.0	805	*x*	γ_{CCH}^{Ph}
1378	0.9	1382	*m*	δ_{CH_3}	788	3.0	780	*x*	δ_{CCC}^{Ph}
1362	146.2			$\nu_{O_1C_4}, \nu_{C_4C_5}$	764	5.7	766	*m*	$\gamma_{O-C=O}$
1336	264.4	1345	*m*	$\delta_{CC1H_1}, \nu_{CC}^{Ph}$	750	65.5	755	*m*	γ_{CCH}^{Coum}
1324	189.7	1329	*m*	$\nu_{NO_2}^{s}$	710	8.3	718	*x*	$\gamma_{O-C=O}$
1318	43.2			ν_{CC}^{Coum}	688	10.3	695	*m*	γ_{CNO}
1299	15.2	1297	*m*	δ_{HCC}^{Ph}	681	19.5	668	*x*	γ_{CCC}^{Ph}
1291	6.4			$\nu_{C_1C_{12}}$	642	4.0	646	*x*	γ_{O_1CC}
1281	59.4	1276	*m*	δ_{CCH_2}	625	1.0	628	*x*	δ_{CO_2C}
1260	25.8			δ_{HCC}^{Coum}	623	0.8	621	*x*	δ_{CCC}^{Ph}
1242	5.8			$\delta_{HCC}^{Coum}, \delta_{CCH_1}$	610	0.5	608	*x*	$\delta_{O-C=O}$
1235	6.5	1214	*m*	$\delta_{CCH_1}, \nu_{CC}^{Coum}$	546	6.4	552	*x*	γ_{CCO_1}
1188	47.9	1199	*m*	$\nu_{O_2C_{10}}$	528	3.9	533	*x*	τ_{CCCH}^{Coum}
1170	114.5	1173	*m*	$\nu_{C-Ph}, \delta_{C_2C_1H_1}$	515	2.7	513	*x*	δ_{CNO}
1165	5.2			δ_{HCC}^{Ph}					

[a]Scaled by 0.9688 [27] .

[b]Vibrational modes: ν, stretching; δ and γ, in-plane and out of plane bending, respectively; τ, torsion
Subscripts: Ph, phenyl ring vibration; Coum, coumarinium ring vibration

The assignment of the experimental bands to the calculated normal modes in the C–H stretching region (3100–2850 cm^{-1}) is not obvious because there are fewer bands in the experimental spectrum than predicted by the calculations. The highest frequency experimental bands observed in the IR spectrum are assigned to the aromatic CH stretches, while the lower frequency bands are attributed to the methyl group motions. The ν(CH) bands are of low intensity in both the experimental and theoretical spectra. In a qualitative agreement between the theory and experiment, the ν(C=O) band is the strongest one in the spectrum. The ν(CO) band, measured at 1716 cm^{-1} in solid state, is sharp, and its frequency is the same as the frequency of the unsubstituted coumarin [33]. These data indicate that the CO group in the studied molecule is free (not involved in hydrogen bond). The strong band at 1627 cm^{-1} has a predominantly C=C character. The frequency and IR intensity of this band is predicted well by theory.

According to the calculation, the strong band observed at 1513 cm^{-1} (calc. 1526 cm^{-1}) in the IR spectrum corresponds to the asymmetric NO_2 mode, while the middle one at 1329 cm^{-1} (calc. 1324 cm^{-1}) is assigned to the symmetric NO_2 mode. The various normal vibrations of the phenyl rings are well shown in the calculated DFT level and are clearly divided into phenyl and coumarin vibrations (Table 5).

Additionally, a very good match was obtained between the calculated and experimental chemical shifts (see Table 6) at the ^{13}C-NMR spectra of **6**. The calculated value of the ^{13}C signal of DMSO-d_6 was 45.3 ppm, which has a difference of 5.8 ppm in comparison with the experimental value (39.5 ppm). That is why the calculated values for the ^{13}C chemical shifts of compound **6** were accordingly corrected.

As a conclusion, using phosphoryl chloride, the hydroxyl group at the acenocoumarol cannot be replaced with a chlorine atom. A dehydration reaction occurs in which the title compound was obtained as a product. The same product was obtained in high yields by performing a dehydration reaction of acenocoumarol with acetic anhydride. The chemical structure of the novel compound was elucidated by a detailed spectroscopic analysis based mainly on 1D and 2D NMR techniques. The structure was finally confirmed with a single-crystal X-ray analysis. The B3LYP/6-311+G** method correctly reproduces the bond lengths, bond angles, torsion angles, and other experimental spectroscopic data, which can be useful for investigating the characteristics of some structurally related molecules.

T a b l e 6

*Calculated (B3LYP/6-311+G**) and experimental ^{13}C-NMR spectral data of 6*

Atom	Calc.	Exp.
C_1	38.0	35.8
C_2	104.3	102.7
C_3	152.6	146.0
C_4	157.0	156.1
C_5	114.6	113.5
C_6	123.4	122.7
C_7	123.3	124.6
C_8	132.7	132.7
C_9	117.2	116.5
C_{10}	155.9	152.2
C_{11}	159.5	160.5
C_{12}	103.9	101.4
C_{21}	152.6	146.3
C_{22}	129.4	129.2
C_{23}	124.3	123.6
C_{24}	149.4	151.9
C_{25}	124.0	123.6
C_{26}	135.2	129.2
C_{31}	15.5	18.0

Supplementary material. Crystallographic data (excluding structure factors) for the structural analysis were deposited with the Cambridge Crystallographic Data Centre, CCDC No. 912247. A copy of this information may be ob-

tained free of charge from the Director, CCDC, 12 Union Road, Cambridge, CB2 1EZ, UK. Fax: +44(1223)336-033, e-mail: deposit@ccdc.cam.ac.uk, or from www.ccdc.cam.ac.uk.

Acknowledgments. This work was supported by the Bulgarian National Science Fund (Contract BM-02/07) and the Macedonian Ministry of Education and Science (Contract 03-1586).

REFERENCES

[1] D. C. Mungra, M. P. Patel, D. P. Rajani, R. G. Patel, Synthesis and identification of b-aryloxyquinolines and their pyrano[3,2-c]chromene derivatives as a new class of antimicrobial and antituberculosis agents, *Eur. J. .Med. Chem.*, **46**, 4192–4200 (2011).

[2] E. Melliou, P. Magiatis, S. Mitaku, A. L. Skaltsounis, E. Chinou, I. Chinou, Natural and synthetic 2,2-dimethylpyranocoumarins with antibacterial activity, *J. Nat. Prod.*, **68**, 78–82 (2005).

[3] A. M. El-Agrody, M. S. Abd El-Latif, N. A. El-Hady, A. H. Fakery, A.H. Bedair, Heteroaromatization with 4-Hydroxycoumarin. Part II: Synthesis of Some New Pyrano[2,3-d]pyrimidines, [1,2,4] triazolo[1,5-c]pyrimidines and Pyrimido[1,6-b]-[1,2,4]triazine Derivatives, *Molecules*, **6**, 519–527 (2001).

[4] M. A. Al-Haiza, M. S. Mostafa, M.Y. El-Kady, Synthesis and Biological Evaluation of Some New Coumarin Derivatives, *Molecules*, **8**, 275–286 (2003).

[5] A. H. Bedair, N. A. El-Hady, M.S. Abd El-latif, A.M. Fakery, A.M. El-Agrody, 4-Hydroxycoumarin in heterocyclic synthesis. Part III. Synthesis of some new pyrano[2,3-d]pyrimidine, 2-substituted[1,2,4] triazolo[1,5-c]pyrimidine and pyrimido[1,6-b] [1,2,4]triazine derivatives, *Farmaco*, **55**, 708–714 (2000).

[6] I. Manolov; N. Danchev, Synthesis and pharmacological investigations of some 4-hydroxycoumarin derivatives, *Archiv der Pharmazie*, **336**, 83–94 (2003).

[7] I. Manolov, C. Maichle-Moessmer, I. Nicolova, N. Danchev, Synthesis and anticoagulant activities of substituted 2,4-diketochromans, biscoumarins, and chromanocoumarins, *Archiv der Pharmazie* (Weinheim, Germany), **339**, 319–326 (2006).

[8] L. Xie, Y. Takeuchi, L. Mark Cosentino, A.T. McPhail, K. H. Lee, Anti-AIDS agents. 42. Synthesis and anti-HIV activity of disubstituted (3′R,4′R)-3′,4′-Di-O-(S)-camphanoyl-(+)-cis-khellactone Analogues, *J. Med. Chem.*, **44**, 664–671 (2001).

[9] K. A. Nolan, H. Zhao, P. F. Faulder, D. A. Frenkel, D. J. Timson, D. Siegel, D, Ross, T. R. Burke, I. J. Stratford, R. A. Bryce, Coumarin-based inhibitors of human NAD(P)H:quinone oxidoreductase-1. Identification, structure-activity, off-target effects and in vitro human pancreatic cancer toxicity, *J. Med. Chem.*, **50**, 6316–6325, (2007).

[10] Y. Jacquot, B. Refouvelet, L. Bermont, G. L. Adessi, G. Leclercq, A. Xicluna, Synthesis and cytotoxic activity of new 2,4-diaryl-4H,5H-pyrano[3,2-c] benzopyran-5-ones on MCF-7 cells, *Pharmazie*, **57**, 233–237 (2002).

[11] W. F. Fong, X. L. Shen, C. Globisch, M. Wiese, G. Y. Chen, G. Y. Zhu, Z. L. Yu, A. K. W. Tse, Y. J. Hu, Methoxylation of 30,40-aromatic side chains improves P-glycoprotein inhibitory and multidrug resistance reversal activities of 7,8-pyranocoumarin against cancer cells, *Bioorg. Med. Chem*., **16**, 3694–3703 (2008).

[12] PATENT; L. Zhu, H. Djaballah, Y. Li, C. C. Shelton, Sloan-kettering institute for cancer research; WO2010/75280; (2010).

[13] C. R. Su, S. F. Yeh, C. M. Liu, A. G. Damu, T.H. Kuo, P. C. Chiang, K. F. Bastow, K. H. Lee, T. S. Wu, Anti-HBV and cytotoxic activities of pyranocoumarin derivatives, *Bioorg. Med. Chem.*, **17**, 6137–6143 (2009).

[14] I. Manolov, C. Maichle-Moessmer, N. Danchev, Synthesis, structure, toxicological and pharmacological investigations of 4-hydroxycoumarin derivatives, *Eur. J. Med. Chem.*, **41**, 882–890 (2006).

[15] PATENT: S. B. Levy, M. N. Alekshun, B. L. Podlogar, K. Ohemeng, A. K. Verma, T. Warchol, B. Bhatia, US2003/229065; (2003).

[16] Y. Liu, J. Zhu, J. Qian, B. Jiang, Z. Xu, Gold(III)-catalyzed tandem conjugate addition/annulation of 4-hydroxycoumarins with α,β-unsaturated ketones, *J. Org. Chem.*, **76**, 9096−9101 (2011).

[17] W. Ma, X. Wang, F. Yan, L. Wu, Y. Wang, Reusable melamine trisulfonic acid-catalyzed three-component synthesis of 7-alkyl-6*H*,7*H*-naphtho[1′,2′:5,6] pyrano[3,2-*c*]chromen-6-ones, *Monatsh Chem.*, **142**, 163–167 (2011).

[18] S. Maiti, S.K. Panja, C. Bandyopadhyay, Synthesis of 6,8-diarylimino-7H-pyrano[3,2-c:5,6-c’]dicoumarins; chemoselective hydrolysis of the ether-and imino-functions, *J. Chem. Res.*, **35**, 84–86 (2011).

[19] H. R. Shaterian, M. Honarmand, Task-specific ionic liquid as the recyclable catalyst for the rapid and green synthesis of dihydropyrano[3,2-c]chromene derivatives, *Syn. Comm.*, **41**, 3573–3581 (2011).

[20] R. Ghorbani-Vaghei, Z. Toghraei-Semiromi, R. Karimi-Nami, One-pot synthesis of 4h-chromene and dihydropyrano[3,2-c]chromene derivatives in hydroalcoholic media, *J. Braz. Chem. Soc*., **22**, 905–909 (2011).

[21] A. T. Khan, M. Lal, S. Ali, Md. M. Khan, One-pot three-component reaction for the synthesis of pyran annulated heterocyclic compounds using DMAP as a catalyst, *Tetrahedron Lett.*, **52**, 5327–5332 (2011).

[22] Agilent (2010) CrysAlis PRO (version 1.171.34.44). Agilent Technologies Ltd, England.

[23] G. M. Sheldrick, A short history of SHELX, *Acta Cryst.* A, **64**, 112–122 (2008).

[24] M. J. Frisch, G. W. Trucks, H. B. Schlegel, G. E. Scuseria, M. A. Robb, J. R. Cheeseman, G. Scalmani, V. Barone, B. Mennucci, G. A. Petersson, H. Nakatsuji, M. Caricato, X. Li, H. P. Hratchian, A. F. Izmaylov, J. Bloino, G. Zheng, J. L. Sonnenberg, M. Hada, M. Ehara, K. Toyota, R. Fukuda, J. Hasegawa, M. Ishida, T. Nakajima, Y. Honda, O. Kitao, H. Nakai, T. Vreven, J. A. Montgomery, Jr., J. E. Peralta, F. Ogliaro, M. Bearpark, J. J. Heyd, E. Brothers, K. N. Kudin, V. N. Staroverov, R. Kobayashi, J. Normand, K. Raghavachari, A. Rendell, J. C. Burant, S. S. Iyengar, J. Tomasi, M. Cossi, N. Rega, J. M. Millam, M. Klene, J. E. Knox, J. B. Cross, V. Bakken, C. Adamo, J. Jaramillo, R. Gomperts, R. E. Stratmann, O. Yazyev, A. J. Austin, R. Cammi, C. Pomelli, J. W. Ochterski, R. L. Martin, K. Morokuma, V. G. Zakrzewski, G. A. Voth, P. Salvador, J. J. Dannenberg, S. Dapprich, A. D. Daniels, Ö. Farkas, J. B. Foresman, J. V. Ortiz, J. Cioslowski, D. J. Fox, Gaussian 09, Revision A1, Gaussian Inc., Wallingford CT, 2009.

[25] A. D. Becke, Density − functional thermochemistry. III. The role of exact exchange, *J. Chem. Phys.*, **98**, 5648–5652 (1993).

[26] C. Lee, W. Yang, G. R. Parr, Development of the Colle-Salvetti conelation energy formula into a functional of the electron density, *Phys. Rev.*, **B37**, 785–791 (1988).

[27] J. P. Merrick, D. Moran, L. Radom, An Evaluation of Harmonic Vibrational Frequency Scale Factors, *J. Phys. Chem*., **A 111**, 11683–11700 (2007).

[28] R. Ditchfield, Self-consistent Perturbation Theory of Diamagnetism. I. A Gauge-Invariant LCAO (Linear Combination of Atomic Orbitals) Method for NMR Chemical Shifts *Mol. Phys*., **27**, 789–807 (1974).

[29] B. Stamboliyska, V. Janevska, B. Shivachev, R. P. Nikolova, G. Stojkovic, B. Mikhova, E. Popovski, Experimental and theoretical investigation of the structure and nucleophilic properties of 4-aminocoumarin, *ARKIVOC*, **(x)**, 62–76 (2010).

[30] R. Sarma, M. M. Sarmah, K. C. Lekhok, D. Prajapati, Organic Reactions in Water: An Efficient Synthesis of Pyranocoumarin Derivatives, *Synlett*., **19**, 2847–2852 (2010).

[31] S. Tu, H. Jiang, F. Fang, Y. Feng, S. Zhu, T. Li, X. Zhang, D. Shi, Synthesis of 2-amino-3-ethoxycarbonyl-4-aryl-4H,5H-pyrano-[3,2-c]benzopyran-5-one. *J. Chem. Res.*, **6**, 396–398 (2004).

[32] Z. He, X. Lin, Y. Zhu, Y. Wang, DDQ-Mediated Tandem Synthesis of Functionalized Pyranocoumarins from 4-Hydroxycoumarins and 1,3-Diarylallylic Compounds. *Heterocycles*, **81**, 965–976 (2010).

[33] Spectral Database for Organic Compounds, *www.aist.go.jp*.